Hindawi
Journal of Nanotechnology
Volume 2019, Article ID 2501039, 11 pages
https://doi.org/10.1155/2019/2501039

Research Article

Preparation and Characterization of Electrospun Gelatin Nanofibers for Use as Nonaqueous Electrolyte in Electric Double-Layer Capacitor

Ditpon Kotatha, Masaharu Hirata, Mayuko Ogino, Satoshi Uchida, Masashi Ishikawa, Tetsuya Furuike, and Hiroshi Tamura

Faculty of Chemistry, Materials and Bioengineering, Kansai University, Osaka 564-8680, Japan

Correspondence should be addressed to Hiroshi Tamura; tamura@kansai-u.ac.jp

Received 31 August 2018; Revised 24 December 2018; Accepted 19 January 2019; Published 24 February 2019

Academic Editor: Oleg Lupan

A novel nanofibrous gel electrolyte was prepared via gelatin electrospinning for use as a nonaqueous electrolyte in electric double-layer capacitors (EDLCs). An electrospinning technique with a 25 wt% gelatin solution was applied to produce gelatin electrospun (GES) nanofiber electrolytes. Structural analysis of the GES products showed a clearly nanofibrous structure with fiber diameters in the 306.2–428.4 nm range and exhibiting high thermal stability, high tensile strength, and a stable form of nanofibrous structure after immersion in 1-ethyl-3-methylimidazolium tetrafluoroborate ($EMImBF_4$). After testing over a range of spinning times, GES electrolytes that were produced at 25 min (GES-25) had a suitable thickness for the assembly of EDLC with the optimized tensile properties and were used to fabricate EDLC test cells with $EMImBF_4$. These test cells were compared to those with pure $EMImBF_4$ and a separator as an electrolyte. The electrochemical properties of the test cells were characterized by charge-discharge testing, discharge capacitance, and alternative current (AC) impedance measurements. AC impedance measurements showed that the test cell with the GES-25/$EMImBF_4$ gel electrolyte showed slightly poorer contact with the electrode when compared to that with pure $EMImBF_4$, whereas exhibited comparable IR drop and discharge capacitance (calculated capacitance retention was 56.6%). The results demonstrated that this novel gel electrolyte can be used as a nonaqueous electrolyte in order to improve the safety in EDLCs.

1. Introduction

Electric double-layer capacitors (EDLCs) represent a class of energy storage devices that can store electrical energy converted from sustainable sources. They are distinguished from other energy storage devices owing to their several unique characteristics such as higher power density with a longer charge-discharge cycle (<100,000 cycles) than rechargeable batteries as well as higher energy density than conventional dielectric capacitors [1–5].

Ionic liquids (ILs) are room-temperature molten salts mostly composed of organic cations and inorganic anions, which are in a liquid state below 100°C, exhibiting nearly unlimited structural diversity and physicochemical variations owing to the appropriate selection and modification of the cations and anions [6]. There are potential alternative electrolytes for EDLCs. Many researchers have been trying to use ILs as solution electrolytes in the EDLCs [7–12] due to their excellent properties such as near-zero vapor pressure, high thermal stability, and nonflammability [13–15]. Nevertheless, liquid leakage and other safety issues limit the application of ILs as electrolytes in EDLCs. Therefore, a nonaqueous electrolyte is a more attractive alternative for EDLCs.

Several nonaqueous electrolytes have been proposed in recent years to satisfy the safety requirements of EDLCs [16–20]. Electrolytes based on natural polymers such as chitosan [21–23], alginate [24–26], agar [27, 28], carrageen

[29–32], starch [33–35], and bacterial cellulose [36] have been widely studied. In addition to being abundant, low cost, nontoxic, and environmentally friendly, natural polymers have been reported to exhibit good physical and mechanical properties and high thermal stabilities.

Gelatin is prepared by the hydrolysis of collagen, which is a natural, triple-helix macromolecule obtained from mammalian skin and bones [37, 38]. Gelatin has been widely used as a scaffold for tissue engineering owing to its excellent biodegradability, biocompatibility, ability to promote cell adhesion and proliferation, and resistance to immunogenicity [39–43]. Moreover, gelatin has the potential to be used as an electrolyte in many applications such as dye-sensitized solar cells and electrochromic devices [44–49].

An important property of gelatin is its gel transition under aqueous conditions. Soluble collagen denatures because of the breakdown of hydrogen and electrostatic bonds in hot water (about 40°C). This process destroys the triple helical structure of collagen to produce one, two, or three random chain gelatin molecules that create a high viscosity solution in water [50, 51]. Gelatin is also compatible with electrospinning, which is a simple and cost-effective technique that is widely used to simply and continuously fabricate nanofibers. Electrospun fibers offer small pores, a high surface area, physical stability, and a controllable thickness in the membrane form [52–54]. Thus, electrospinning is an attractive option for fabricating gel electrolytes to apply in EDLCs.

In this study, we fabricated a novel electrolyte from gelatin via an electrospinning technique. We focused on one potential application of the electrolyte in EDLCs for improved device safety. The novel gelatin electrospun (GES) nanofiber electrolyte included ionic liquid of 1-ethyl-3-methylimidazolium ($EMImBF_4$), which has high ionic conductivity and low viscosity and is widely used as an electrolyte in EDLCs [8–10]. The electrochemical properties of the EDLC test cells assembled with the novel electrolyte were characterized and measured with respect to the charge-discharge characteristics, discharge capacitance, and AC impedance.

2. Materials and Methods

2.1. Materials. Gelatin (JS200, Mw = 100,000, bovine skin type B, Lot No. 120705M) was purchased in powder form from Koei Chemical Co., Ltd (Japan), and 1-ethyl-3-methylimidazolium tetrafluoroborate ($EMImBF_4$, 99.0%) was purchased from Toyo Gosei Co., Ltd (Japan). Activated carbon (YP-50F), acetylene black (HS-100), sodium carboxymethyl cellulose (WS-C), and styrene-butadiene rubber (TRD2001) were purchased from Kuraray Co., Ltd (Japan), Denka company Ltd (Japan), DKS Co., Ltd (Japan), and JSR corporation (Japan), respectively.

2.2. Preparation of GES Electrolytes. 25 wt% gelatin powder was dissolved in deionized (DI) water, and the mixture was stirred at 50°C until a homogeneous solution was obtained. The solution was maintained in a water bath at 50°C for approximately 1 h to remove entrapped air and then cooled in an ice bath to induce gelation. The gelated gelatin was placed in a 5 mL syringe with a metal needle of diameter 1.5 mm, and the syringe was placed in a water bath at 50°C to reverse the gelation; the temperature of the syringe was thereafter maintained at 45°C–50°C. A high-voltage power supply of 23 kV was connected to the syringe needle tip and to a stationary collector covered with an aluminum foil. The tip-to-collector distance was set at 7 cm. The electrospun nanofibers were collected as randomly overlaid mats on the electrically grounded plate. The spinning time was varied between 5, 10, 15, 20, and 25 min. The GES samples were dried at 25°C (room temperature) under ambient conditions for 12 h before being removed from the aluminum foil; the dried sample was placed in a desiccator containing a silica-gel desiccant before being used for further testing. In addition, the selected GES sample was soaked in $EMImBF_4$ under 0.3 Pa vacuum at room temperature for 48 h before EDLC test cells fabrication.

2.3. Characterization

2.3.1. Fourier Transform Infrared Spectroscopy (FTIR). Fourier transform infrared spectroscopy (FTIR; 670-IR, VARIAN Inc., USA) was used for the identification of the functional groups in the samples. All FTIR spectra were scanned with a resolution of 0.5 cm^{-1} in the 4000–400 cm^{-1} range.

2.3.2. Thermogravimetric/Differential Thermal Analysis (TG/DTA). Thermogravimetric/differential thermal analysis was performed by a TG/DTA analyzer (EXSTAR TG/DTA6200, SII, Japan) in order to measure the thermal properties of the samples. All samples were vacuum dried at room temperature for one day before analysis. The samples were tested at a heating rate of 20°C/min in the 30°C–500°C range under a nitrogen atmosphere.

2.3.3. Differential Scanning Calorimetry (DSC). Differential scanning calorimetry (DSC; EXSTAR DSC6220, SII, Japan) was conducted using a sample in an aluminium pan that was hermetically sealed. The samples were tested at a heating rate of 20°C/min in the 30°C–350°C range under a nitrogen atmosphere.

2.3.4. Scanning Electron Microscopy (SEM). The morphologies of the obtained samples were analyzed via scanning electron microscopy (SEM; JSM6700, JEOL, Japan) at an accelerating voltage of 5 kV with 500 × and 2000 × magnification, and the diameter and size distribution of the fibers were analyzed by using image visualization software (Image-Pro Plus).

2.3.5. GES Membrane Thickness and Mechanical Properties. The mechanical properties of the samples were analyzed using a universal testing machine (STA-1150, A&D Company, Ltd, Japan) equipped with a 50-N load cell and elongated at a constant speed of 10 mm/min under ambient conditions. The

test samples were cut to 30 mm in length and 5 mm in width and were mounted in the tensile grips spaced 10 mm apart before analysis. The thicknesses of the samples were measured by a digital micrometer (IP65, Mitutoyo, Japan).

2.4. Fabrication of EDLC Test Cells. Composite carbon electrodes were prepared by mixing activated carbon (YP-50F), acetylene black (HS-100) as a conductive additive, 1.2 wt% sodium carboxymethyl cellulose (WS-C) as a dispersant, and 48 wt% styrene-butadiene rubber (TRD2001) as a binder in DI water at a ratio of 90 : 5:3 : 2 (w/w). The slurry was then cast onto an etched aluminium-foil current collector and dried; the obtained composite electrode sheet was cut into 12 mm diameter disks. Two carbon electrodes were immersed in $EMImBF_4$ for 10 min in a glove box under reduced pressure while the gel electrolyte was soaked in $EMImBF_4$ under a 0.3 Pa vacuum at room temperature for 48 h. The test cells were then assembled with the prepared carbon electrodes and gel electrolytes in a coin cell (CR2023, stainless type, Hohsen Corporation, Japan). In addition, test cells were assembled with liquid-phase $EMImBF_4$ and a cellulose separator (TF4035, Nippon Kodoshi Corporation, Japan) for comparison. The whole assembly procedure was performed in an argon-filled glove box.

2.5. Measurement of Electrochemical Properties. The electrochemical properties of EDLC test cells were measured in terms of the charge-discharge characteristics, discharge capacitance, and AC impedance of each test cell. The performance was measured using a battery charge/discharge apparatus (HJ1001 SM8, Hokuto Denko Corporation, Japan). The charge-discharge tests were carried out in the voltage range from 0 to 2.5 V at various densities. The discharge rate was estimated at various discharge current densities between 2.5 and 100 mA/cm^2 when a constant current was charged up to 2.5 V. The discharge capacitance of a single electrode in the EDLC symmetrical cells was determined using equation (1) [21–25]:

$$C = \left(\frac{I \times t}{(V/2) \times W} \right), \quad (1)$$

where C is the discharge capacitance (F/g), I is the discharge current (A), t is the discharge time (s), V is the operating voltage (V), and W is the total mass of activated carbon in a single electrode (g).

AC impedance measurements were performed using a potentiogalvanostat (SI 1287 type, Solartron Analytical, UK) and a frequency-response analyzer (SI 1260 type, Solartron Analytical, UK) with an AC amplitude of 10 $mV_{p\text{-}0}$ in the frequency range of 500 kHz–10 mHz. All electrochemical measurements were performed at 25°C.

3. Results and Discussion

3.1. Characterization

3.1.1. FTIR. The FTIR spectra of gelatin powder and GES fibers fabricated at spinning times of 5, 10, 15, 20, and 25 min (labeled as GES-5, GES-10, GES-15, GES-20, and GES-25, respectively) are shown in Figure 1(a). All samples showed similar absorption peaks. The characteristic peaks were interpreted as follows: the peak around 3300 cm^{-1} is due to the stretching vibration of N–H (amide A) and hydrogen bonding. The peak at 1650 cm^{-1} corresponds to the stretching vibration of C=O (amide I). The peak at 1540 cm^{-1} is induced by the bending and stretching vibration of N–H (amide II), and the peak at 1240 cm^{-1} is attributed to the bending of N–H. These absorption peaks are characteristic of gelatin [39, 55]; therefore, the presence of these peaks proves that the electrospinning process did not alter the functional groups of the gelatin.

In addition, the GES-25 sample after immersion in $EMImBF_4$ before the EDLC fabrication process (GES-25/$EMImBF_4$) was measured by FTIR spectra for comparison with GES-25 and $EMImBF_4$. The results are shown in Figure 1(b). The adsorption peak for GES-25/$EMImBF_4$ is similar to that of GES-25 except for the new characteristic peaks of $EMImBF_4$, which were observed as follows: the peaks at 3140 and 2980 cm^{-1} are due to the aliphatic asymmetric and symmetric C–H stretching vibrations (imidazolium ring). The peak at 1570 cm^{-1} is attributed to the C=C stretching vibration (imidazolium ring). The peak at 1169 cm^{-1} is induced by the C–N stretching vibration (imidazolium ring), and the peaks at 1049 and 525 cm^{-1} correspond to the asymmetric vibration of B–F [56–59]. The results confirm that $EMImBF_4$ was introduced into the GES nanofibers.

3.1.2. TG/DTG. TG and DTG thermograms of gelatin powder, GES products, GES-25/$EMImBF_4$, and $EMImBF_4$ are shown in Figures 2(a) and 2(b), respectively. The gelatin powder and all GES products including the GES-25/$EMImBF_4$ sample demonstrated weight loss due to the evaporation of the moisture on the surface in the temperature range of 40°C–130°C. The moisture content of the GES products was higher than that of the gelatin powder because of the comparatively high surface area of the GES fibers. The gelatin powder and all GES products showed only one thermal degradation step at which the onset of weight loss occurred around 200°C and the maximum weight loss occurred at approximately 330°C due to protein degradation [60, 61]. In contrast, the GES-25/$EMImBF_4$ sample showed two distinctive thermal degradation stages. The first stage was observed at a temperature similar to that of gelatin powder and all GES products due to the degradation of the protein. The second stage was observed at 423°C due to the decomposition of $EMImBF_4$ [62]; this can be seen also in the TG and DTG results for pure $EMImBF_4$. These results demonstrate a high thermal stability and imply that GES fibers may potentially be used as gel electrolytes in EDLCs under high-temperature operations.

3.1.3. DSC. DSC determination grants information about the possible interactions between components in the target matrix, thereby providing knowledge about the applicability and stability of the biopolymer [63]. The DSC curves of

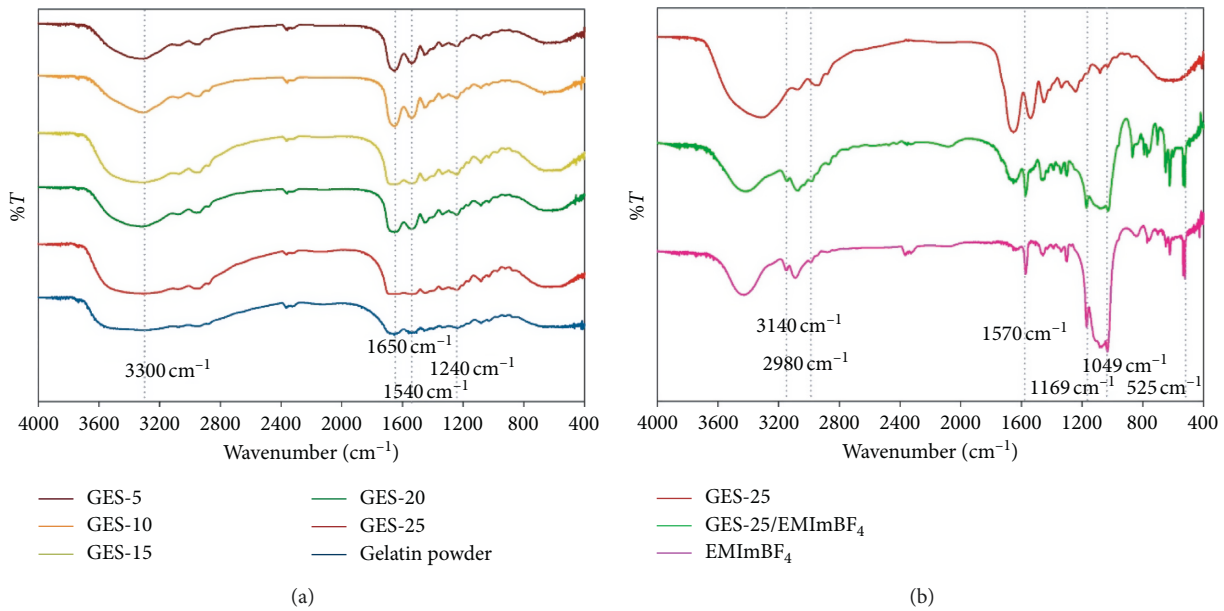

Figure 1: FTIR spectra of (a) gelatin powder and GES products and (b) GES-25, GES-25/$EMImBF_4$, and $EMImBF_4$.

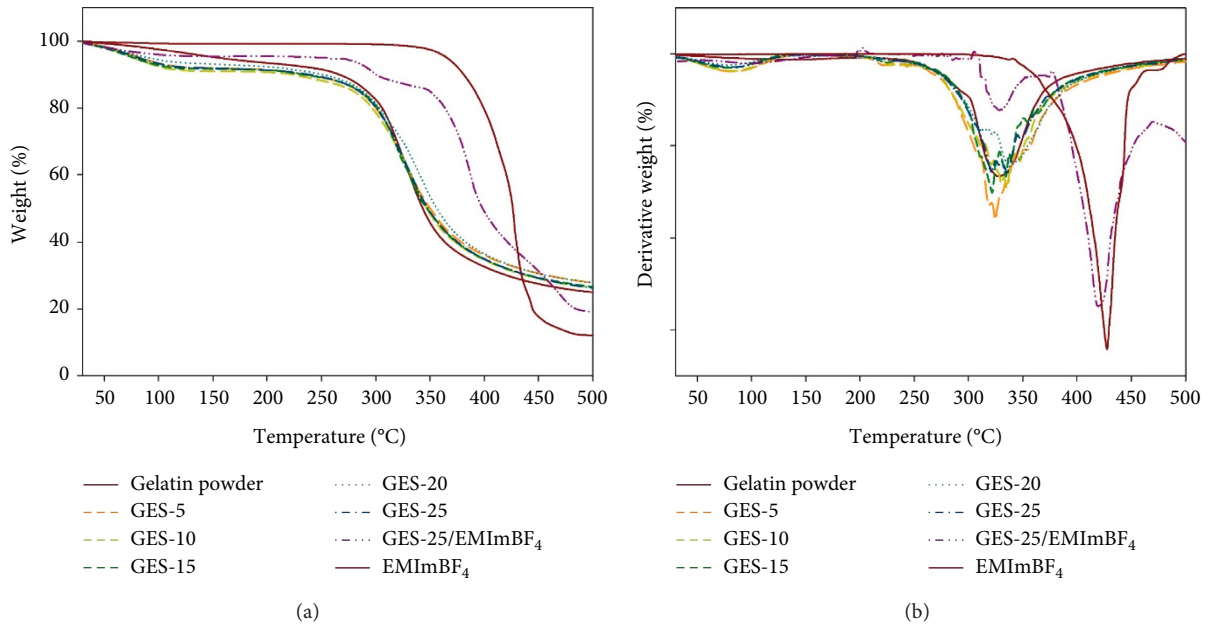

Figure 2: (a) TGA and (b) DTG thermograms of gelatin powder, GES products, GES-25/$EMImBF_4$, and $EMImBF_4$.

gelatin powder, GES-25, and GES-25/$EMImBF_4$ are shown in Figures 3(a)–3(c), respectively. The DSC curves represent an endothermic peak related to the glass transition temperature (T_g), the melting temperature (T_m), and the degradation temperature ($T_{degradation}$) of the samples. The T_g of gelatin powder and GES-25 were found to be 72.9°C, while the T_g of GES-25/$EMImBF_4$ was found to be 82.5°C. It is therefore possible that this observation is due to $EMImBF_4$ incorporated into the GES fiber. The T_m and $T_{degradation}$ of gelatin powder, GES-25, and GES-25/$EMImBF_4$ were found to be approximately 110°C and 277°C, respectively. The values of T_g/T_m and $T_{degradation}$ are in agreement with the values reported in the literature [51, 64]. Hence, the GES nanofibers could withstand the high temperatures; this result was consistent with the results of TG/DTG.

3.1.4. SEM. SEM images of the GES products, as well as the fiber-diameter distribution measured from the SEM images, are shown in Figure 4. The SEM images revealed a clearly nanofibrous structure with an average fiber diameter in the 306.2–428.4 nm range. The spinning time was not affected by the average diameter size of the fiber. The average diameter size of GES-5, GES-10, GES-15, GES-20, and GES-25 was 350.2, 332.1, 306.1, 320.1, and 428.4 nm, respectively.

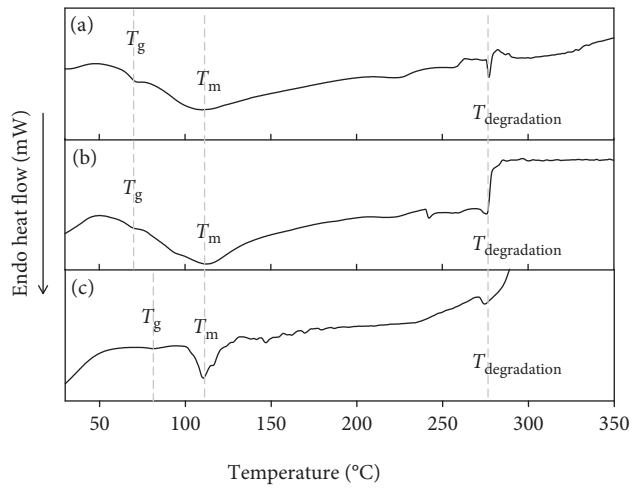

Figure 3: DSC curves of (a) gelatin powder, (b) GES-25, and (c) GES-25/EMImBF$_4$.

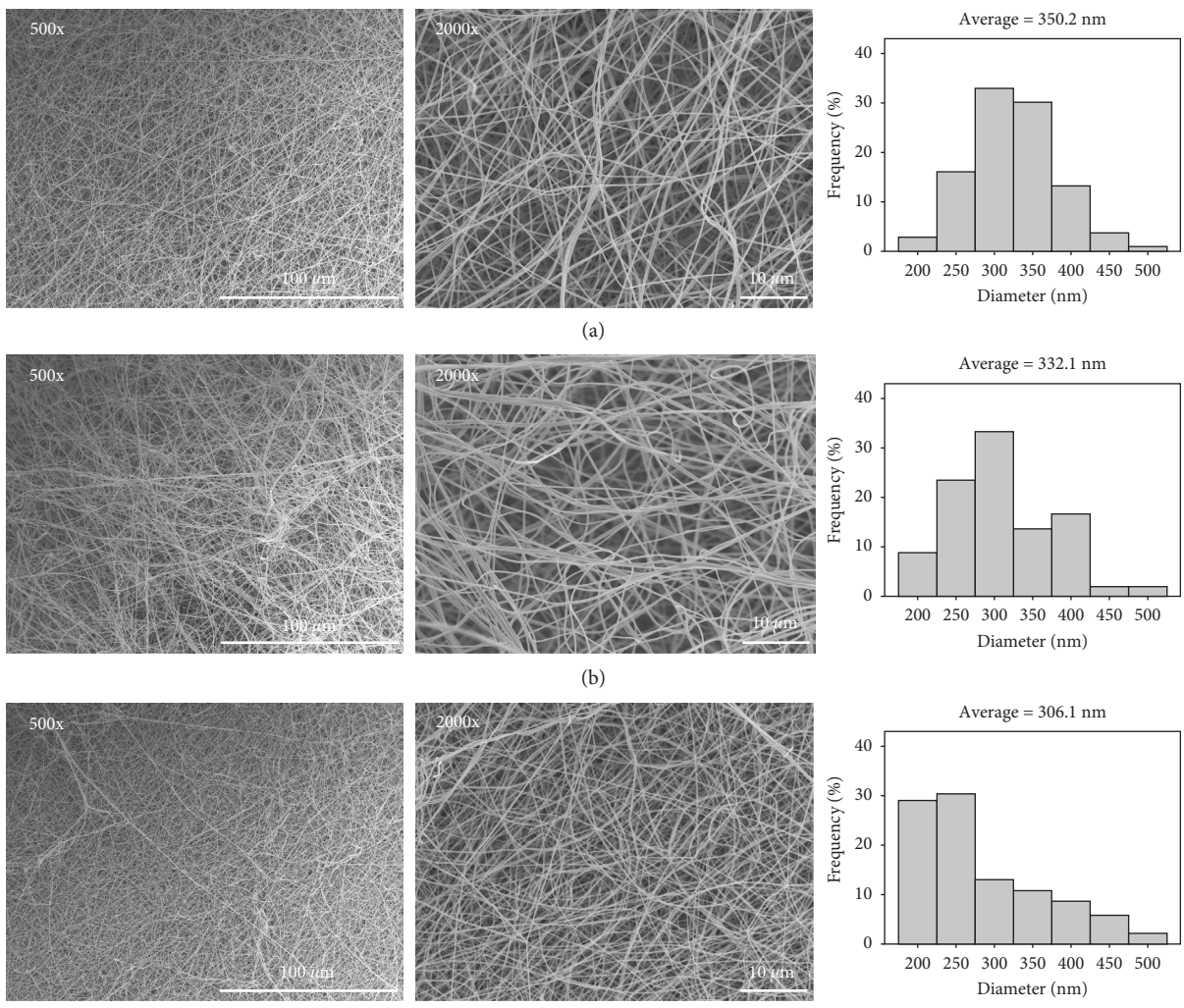

Figure 4: Continued.

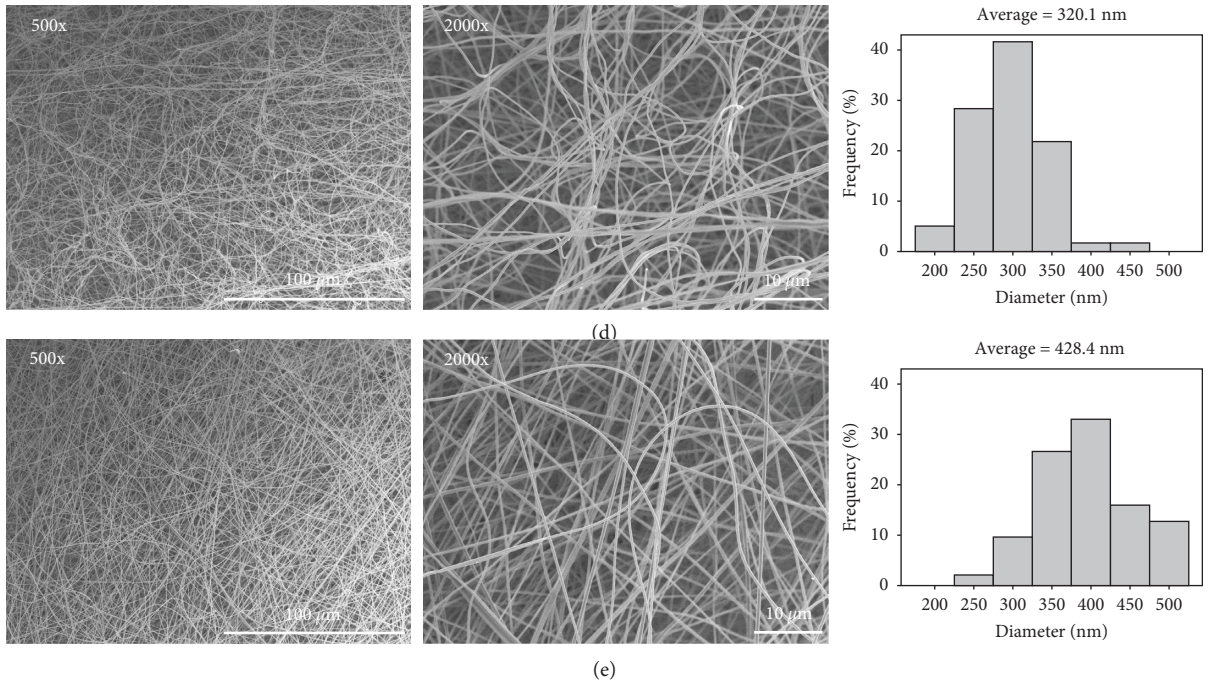

Figure 4: SEM images with 500 × and 2000 × magnification and the measured fiber-diameter distribution of (a) GES-5, (b) GES-10, (c) GES-15, (d) GES-20, and (e) GES-25.

3.1.5. GES Membrane Thickness and Mechanical Properties. The thickness, tensile strength, and % elongation at break of the GES products are shown in Table 1. The thicknesses of the membranes were greater with higher spinning times. This result is consistent with the tensile strength results: the tensile strength was greater in membranes fabricated with higher spinning times. On the contrary, the elongation at break of the GES products showed no tendency to increase or decrease with the spinning time, exhibiting an average of 13% elongation at break. This may have been due to the fibrous structure of the samples. Based on these results, the GES-25 sample showed the highest tensile strength with a thickness that was suitable for its use as a gel electrolyte in EDLCs. Thus, GES-25 was chosen for the following electrochemical tests.

3.1.6. Effect of $EMImBF_4$ on GES. GES-25 after immersion in $EMImBF_4$ before the EDLC fabrication process (GES-25/$EMImBF_4$; wet stage) was compared with GES-25 (dry stage) to evaluate its mechanical properties. The results are shown in Table 2. The tensile strength of GES-25/$EMImBF_4$ was decreased, while the elongation at break was obviously enhanced compared to GES-25. It is well known that gelatin nanofibrous membrane tends to be rubber-like in the wet stage and rigid-brittle in the dry stage [65]. This was mainly attributed to the presence of the $EMImBF_4$ solution dispersed in the pores of nanofibrous membrane, thus weakening the interaction among neighboring fibers [66, 67].

Furthermore, the GES-25/$EMImBF_4$ sample was continually immersed in $EMImBF_4$ at room temperature, incubated in a desiccator for 10 days, and washed with ethanol. Then, the structural morphology of this sample was observed using SEM as shown in Figure 5. The results indicated that the nanofibers of GES-25/$EMImBF_4$ were stable and were not deformed from a fibrous structure after continuous immersion in $EMImBF_4$ at room temperature for 10 days. It was reasonably explained that the GES nanofibers may potentially serve as a host to $EMImBF_4$.

3.1.7. Electrochemical Results. The electrochemical properties of the EDLC test cell with the GES-25/$EMImBF_4$ gel electrolyte were measured and compared with the liquid phase of $EMImBF_4$ as the electrolyte.

Table 1: Thickness and mechanical properties of GES products.

Sample	Thickness (μm)	Tensile strength (cN)	Elongation at break (%)
GES-5	25.5 ± 3.8	29.6 ± 11.6	11.6 ± 3.0
GES-10	34.8 ± 5.6	50.2 ± 22.5	11.3 ± 4.5
GES-15	46.1 ± 6.2	78.2 ± 35.0	14.5 ± 4.2
GES-20	72.4 ± 9.3	90.4 ± 24.5	13.3 ± 4.1
GES-25	76.4 ± 8.8	147.3 ± 33.7	15.8 ± 3.0

Table 2: Comparison of the mechanical properties of GES-25/$EMImBF_4$ and GES-25.

Sample	Tensile strength (cN)	Elongation at break (%)
GES-25 (dry stage)	147.3 ± 33.7	15.8 ± 3.0
GES-25/$EMImBF_4$ (wet stage)	30.8 ± 6.1	47.3 ± 5.5

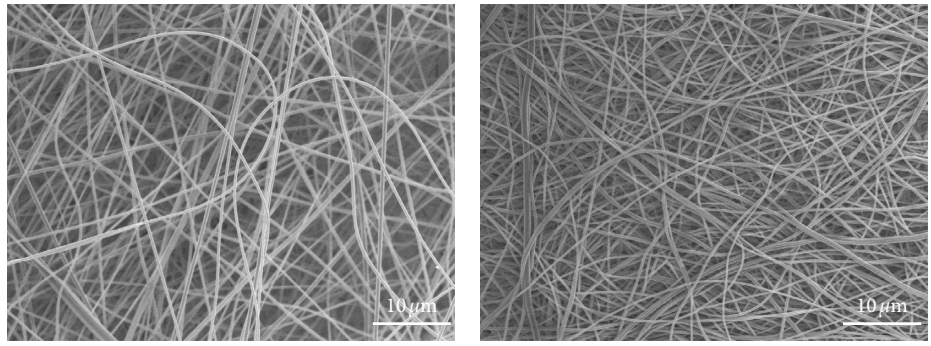

(a) (b)

Figure 5: SEM images of (a) GES-25 and (b) GES-25/$EMImBF_4$ after continuous immersion in $EMImBF_4$ for 10 days.

The charge-discharge curves of EDLC test cells assembled with liquid-phase $EMImBF_4$ and GES-25/$EMImBF_4$ were measured at high current densities of 50 and 100 mA/cm^2 and are shown in Figures 6(a) and 6(b), respectively. Under these high current densities, the test cell with the GES-25/$EMImBF_4$ gel electrolyte showed an IR drop at the switching point from charge to discharge, which was slightly larger than the IR drop of the test cell with liquid-phase $EMImBF_4$ due to the ionic conductivity of the test cell with GES-25/$EMImBF_4$ being lower than that of the liquid-phase $EMImBF_4$ system [36, 68]. However, the ionic conductivity of the test cell with GES-25/$EMImBF_4$ was shown to be significantly higher than that of the conventional gel-electrolytes composed of synthesized polymer matrix from previous reports [69].

In addition, the discharge capacitance of the same EDLC test cells as a function of the applied current density in the range of 2.5–100 mA/cm^2 is shown in Figure 7. The results demonstrate that the discharge capacitance retention of the test cell with the GES-25/$EMImBF_4$ gel electrolyte differed only slightly from that of the test cell with the liquid-phase $EMImBF_4$ electrolyte, within the entire current-density range. The calculated capacitance retention from the initial current density of 2.5 to 100 mA/cm^2 of the test cells with GES-25/$EMImBF_4$ was 56.6% which is comparable with the test cell using natural polymer gel electrolytes from chitosan, alginate, or bacterial cellulose including $EMImBF_4$ from previous reports [25, 36, 68]. As a result, it should be noted that GES-25/$EMImBF_4$ has the potential to exhibit an excellent electrochemical performance in the EDLC cell.

Overall, the charge-discharge measurements indicate that GES-25/$EMImBF_4$ may be more effective as an electrolyte than liquid-phase $EMImBF_4$ in nonaqueous EDLCs for improving the safety of the devices without reducing the performance.

AC impedance measurements were carried out on the EDLC test cells assembled with either liquid-phase $EMImBF_4$ or the GES-25/$EMImBF_4$ electrolytes for the investigation of the electrochemical behavior at the electrode/electrolytes interface in detail [36, 68]. The Nyquist plots obtained by AC impedance measurements on the test cells having liquid-phase $EMImBF_4$ or GES-25/$EMImBF_4$ as electrolytes are shown in Figure 8. Both test cells showed a small semicircle at high frequencies followed by a transition to linearity at low frequencies, corresponding to capacitive behavior [69, 70]. Focusing on the semicircles, which represent the contact resistance between an electrode and electrolytes of the test cell [25, 36, 69, 71]; the observed semicircle of the test cell with GES-25/$EMImBF_4$ was slightly larger than test cells with liquid-phase $EMImBF_4$. This result indicates that the obtained GES electrolyte was in poor contact with the activated carbon electrode [36, 68]. Thus, to improve the contact surface between the GES gel electrolyte and the electrode of activated carbon is an interesting topic for future research. However, the knowledge gained from this experiment has the potential to guide future approaches to develop gel electrolytes from gelatin for use in EDLCs.

4. Conclusions

In this study, a novel nonaqueous gel electrolyte was successfully prepared by electrospinning of gelatin and characterized to evaluate its application as both the electrolyte and the separator for EDLCs. To fabricate the electrolytes, gelatin powder was dissolved in DI water at 25 wt%. This solution was then electrospun over a range of spinning times. Based on structural analysis, the fabricated GES electrolytes had a nanofibrous structure with fiber diameters in the 306.2–428.4 nm range. The FTIR spectra of the GES products revealed peaks that are characteristic of gelatin, indicating that the electrospinning process did not alter the functional groups of the gelatin. TG/DTG and DSC curves indicated that the GES products had high thermal stabilities, which is a favorable property for gel electrolytes used in EDLCs at high-temperature operation. The thickness of the GES membranes increased with an increase in spinning time. The tensile test results for the obtained samples showed that the nanofibrous structure was highly flexible and had a high tensile strength. Moreover, the GES-25/$EMImBF_4$ sample before fabricating in the EDLC was characterized; FTIR, TG/DTG, and DSC results indicated that $EMImBF_4$ was dispersed in the pores of the GES nanofibers. The mechanical properties showed a decrease in tensile strength and an increase in % elongation

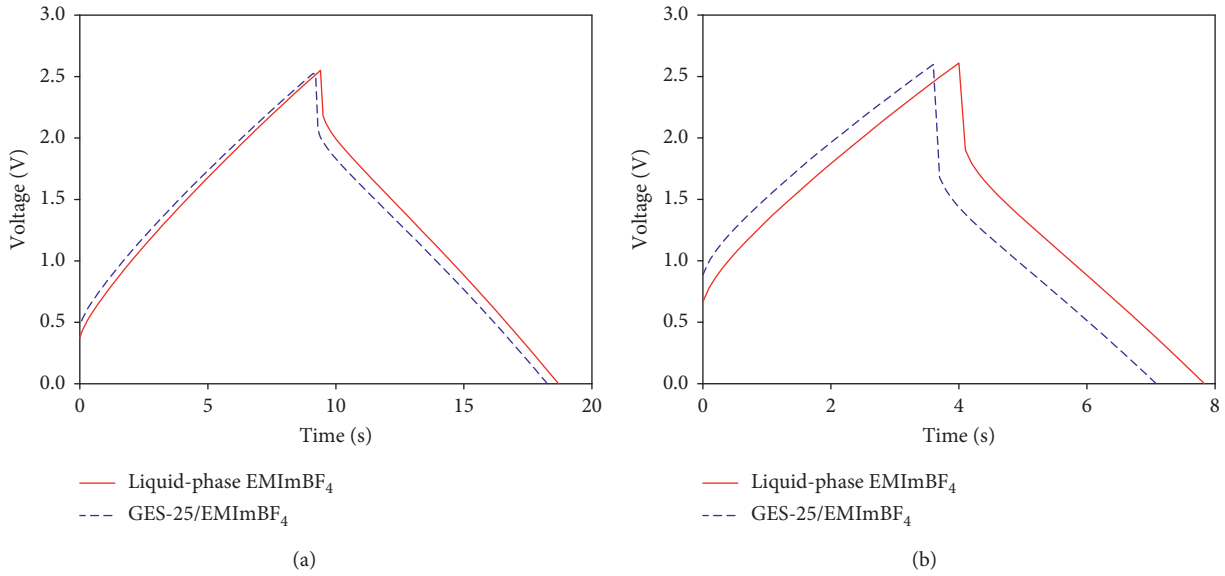

Figure 6: Charge-discharge curves of the EDLC test cells with liquid-phase $EMImBF_4$ and with GES-25/$EMImBF_4$ as the electrolytes at current densities of (a) 50 and (b) 100 mA/cm^2.

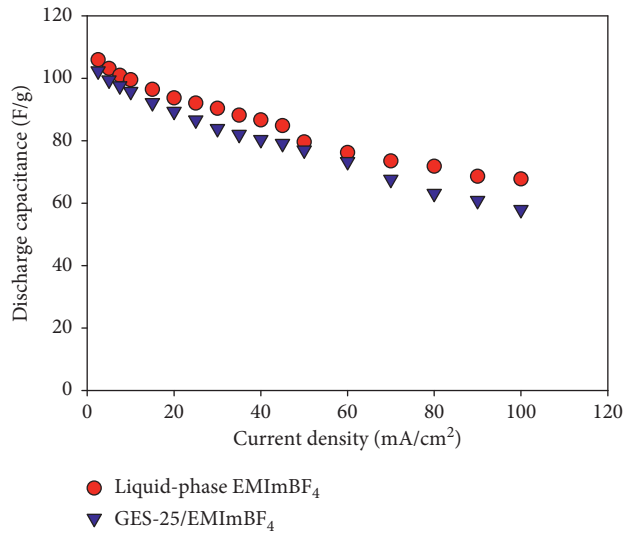

Figure 7: Discharge capacitance of the EDLC test cells with liquid-phase $EMImBF_4$ and with GES-25/$EMImBF_4$ as the electrolytes.

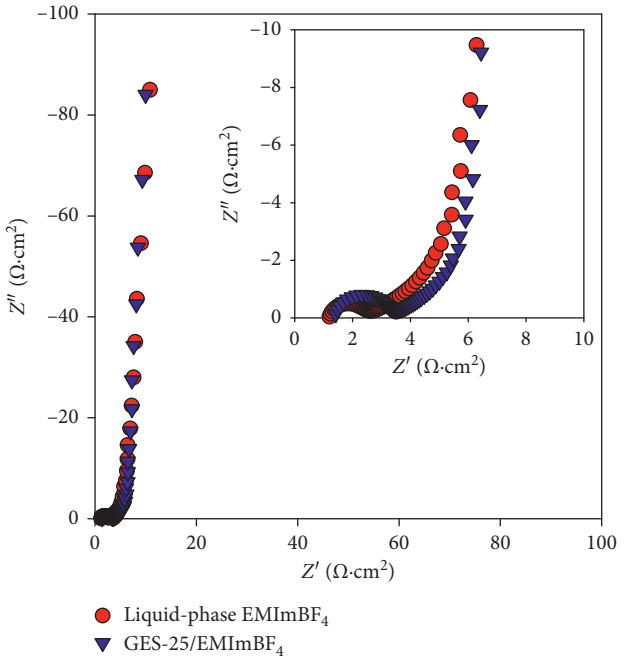

Figure 8: Nyquist plots obtained by AC impedance measurements of EDLC test cells with liquid-phase $EMImBF_4$ and with GES-25/$EMImBF_4$ as electrolytes.

at break and showed a stable form of nanofibrous structure after immersion in $EMImBF_4$.

EDLC test cells were assembled with GES-25/$EMImBF_4$ and with pure $EMImBF_4$ as the electrolytes to evaluate their electrochemical properties. The test cell with the GES-25/$EMImBF_4$ gel electrolyte exhibited a comparable IR drop and discharge capacitance as compared to that with liquid-$EMImBF_4$. The GES-25/$EMImBF_4$-assembled test cell also showed a poor electrode/gel electrolyte interface resistance at the electrode/electrolyte interface compared to those with pure $EMImBF_4$ electrolytes. The electrochemical characteristics suggested that the proposed novel electrolyte of GES nanofibers can be employed as an effective nonaqueous gel electrolyte in EDLCs, thereby improving the safety of such devices.

Data Availability

The data used to support the findings of this study are available from the corresponding author upon request.

Disclosure

An earlier shot-version of this research has been presented as conference abstract in 2nd International Conference on

Engineering and Technology for Sustainable Development (ICET4SD).

Conflicts of Interest

The authors declare that there are no conflicts of interest regarding the publication of this paper.

Acknowledgments

This work was financially supported in part by the Kansai University Fund for the Promotion and Enhancement of Education and Research, 2017 "Development of Environmental Friendly Functional Materials," the Kansai University Outlay Support for Establishing Research Centers (2016–2017), and the Private University Research Branding Project: Matching Fund Subsidy from the Ministry of Education, Culture, Sports, Science and Technology (MEXT), Japan (2016–2020).

References

[1] P. Sharma and T. S. Bhatti, "A review on electrochemical double-layer capacitors," *Energy Conversion and Management*, vol. 51, pp. 2901–2912, 2010.

[2] M. Winter and R. J. Brodd, "What are batteries, fuel cells, and supercapacitors?," *Chemical Reviews*, vol. 104, no. 10, pp. 4245–4269, 2004.

[3] M. Galiński, A. Lewandowski, and I. Stępniak, "Ionic liquids as electrolytes," *Electrochimica Acta*, vol. 51, pp. 5567–5580, 2006.

[4] S. Yoon, J. Lee, T. Hyeon, and S. M. Oh, "Electric double-layer capacitor performance of a new mesoporous carbon," *Journal of the Electrochemical Society*, vol. 147, no. 7, pp. 2507–2512, 2000.

[5] M. Tokita, N. Yoshimoto, K. Fujii, and M. Morita, "Degradation characteristics of electric double-layer capacitors consisting of high surface area carbon electrodes with organic electrolyte solutions," *Electrochimica Acta*, vol. 209, pp. 210–218, 2016.

[6] V. L. Martins and R. M. Torresi, "Ionic liquids in electrochemical energy storage," *Current Opinion in Electrochemistry*, vol. 9, pp. 26–32, 2018.

[7] A. Lewandowski and M. Galiński, "Carbon–ionic liquid double-layer capacitors," *Journal of Physics and Chemistry of Solids*, vol. 65, no. 2-3, pp. 281–286, 2004.

[8] Z. Zhou, M. Takeda, and M. Ue, "New hydrophobic ionic liquids based on perfluoroalkyltrifluoroborate anions," *Journal of Fluorine Chemistry*, vol. 125, no. 3, pp. 471–476, 2004.

[9] T. Sato, G. Masuda, and K. Takagi, "Electrochemical properties of novel ionic liquids for electric double layer capacitor applications," *Electrochimica Acta*, vol. 49, no. 21, pp. 3603–3611, 2004.

[10] K. Yuyama, G. Masuda, H. Yoshida, and T. Sato, "Ionic liquids containing the tetrafluoroborate anion have the best performance and stability for electric double layer capacitor applications," *Journal of Power Sources*, vol. 162, no. 2, pp. 1401–1408, 2006.

[11] C. O. Ania, J. Pernak, F. Stefaniak, E. Raymundo-Piñero, and F. Béguin, "Solvent-free ionic liquids as *in situ* probes for assessing the effect of ion size on the performance of electrical double layer capacitors," *Carbon*, vol. 44, no. 14, pp. 3113–3148, 2006.

[12] S. Yamazaki, T. Ito, M. Yamagata, and M. Ishikawa, "Non-aqueous electrochemical capacitor utilizing electrolytic redox reactions of bromide species in ionic liquid," *Electrochimica Acta*, vol. 86, pp. 294–297, 2012.

[13] X. Mu, X. Yang, D. Zhang, and C. Liu, "Theoretical study of the reaction of chitosan monomer with 2,3-epoxypropyltrimethyl quaternary ammonium chloride catalyzed by an imidazolium-based ionic liquid," *Carbohydrate Polymers*, vol. 146, pp. 46–51, 2016.

[14] W. Wang, J. Zhu, X. Wang, Y. Huang, and Y. Wang, "Dissolution behavior of chitin in ionic liquids," *Journal of Macromolecular Science, Part B*, vol. 49, no. 3, pp. 528–541, 2010.

[15] K. Wilpiszewska and T. Spychaj, "Ionic liquids: media for starch dissolution, plasticization and modification," *Carbohydrate Polymers*, vol. 86, no. 2, pp. 424–428, 2014.

[16] B. Rupp, M. Schmuck, A. Balducci, M. Winter, and W. Kern, "Polymer electrolyte for lithium batteries based on photochemically crosslinked poly(ethylene oxide) and ionic liquid," *European Polymer Journal*, vol. 44, no. 9, pp. 2986–2990, 2008.

[17] M. Rao, X. Geng, Y. Liao, S. Hu, and W. Li, "Preparation and performance of gel polymer electrolyte based on electrospun polymer membrane and ionic liquid for lithium ion battery," *Journal of Membrane Science*, vol. 399-400, pp. 37–42, 2012.

[18] P. F. R. Ortega, J. P. C. Trigueiro, G. G. Silva, and R. L. Lavall, "Improving supercapacitor capacitance by using a novel gel nanocomposite polymer electrolyte based on nanostructured SiO_2, PVDF and imidazolium ionic liquid," *Electrochimica Acta*, vol. 188, pp. 809–817, 2016.

[19] M. Safa, A. Chamaani, N. Chawla, and B. El-Zahab, "Polymeric ionic liquid gel electrolyte for room temperature battery applications," *Electrochimica Acta*, vol. 213, pp. 587–593, 2016.

[20] J. Rymarczyk, M. Carewska, G. B. Appetcchi et al., "A novel ternary polymer electrolyte for LMP batteries based on thermal cross-linked poly(urethane acrylate) in presence of a lithium salt and an ionic liquid," *European Polymer Journal*, vol. 44, no. 7, pp. 2153–2161, 2008.

[21] K. Soeda, M. Yamagata, S. Yamazaki, and M. Ishikawa, "Application of chitosan-based gel electrolytes with ionic liquids for high-performance and safe electric double layer capacitors," *Electrochemistry*, vol. 81, no. 10, pp. 867–872, 2013.

[22] M. Yamagata, K. Soeda, S. Ikebe, S. Yamazaki, and M. Ishikawa, "Chitosan-based gel electrolyte containing an ionic liquid for high-performance nonaqueous supercapacitors," *Electrochimica Acta*, vol. 100, pp. 275–280, 2013.

[23] M. Yamagata, K. Soeda, S. Ikebe, S. Yamazaki, and M. Ishikawa, "Polysaccharide-based gel electrolyte containing hydrophobic ionic liquids for electric double-layer capacitors," *Journal of the Electrochemical Society*, vol. 41, no. 22, pp. 25–35, 2012.

[24] M. Yamagata, S. Ikebe, Y. Kasai, K. Soeda, and M. Ishikawa, "Dramatic improvements in electric double-layer capacitors using polysaccharides," *ECS Transactions*, vol. 50, no. 43, pp. 27–36, 2013.

[25] K. Soeda, M. Yamagata, and M. Ishikawa, "Outstanding features of alginate-based gel electrolyte with ionic liquid for electric double layer capacitors," *Journal of Power Sources*, vol. 280, pp. 565–572, 2015.

[26] M. Yamagata, K. Soeda, S. Yamazaki, and M. Ishikawa, "Charge-discharge behaviour of electric double layer

capacitor with alginate/ionic liquid gel electrolyte," *Journal of Electrochemical Society*, vol. 25, no. 35, pp. 193–200, 2010.

[27] E. Raphael, C. O. Avellaneda, B. Manzolli, and A. Pawlicka, "Agar-based films for application as polymer electrolytes," *Electrochimica Acta*, vol. 55, no. 4, pp. 1455–1459, 2010.

[28] R. Leones, F. Sentanin, L. C. Rodrigues et al., "Investigation of polymer electrolytes based on agar and ionic liquids," *Express Polymer Letters*, vol. 6, no. 12, pp. 1007–1016, 2012.

[29] S. Rudhziah, M. S. A. Rani, A. Ahmad, N. S. Mohamed, and H. Kaddami, "Potential of blend of kappa-carrageenan and cellulose derivatives for green polymer electrolyte application," *Industrial Crops and Products*, vol. 72, pp. 133–141, 2015.

[30] N. N. Mobarak, N. Ramli, A. Ahmad, and M. Y. A. Rahman, "Chemical interaction and conductivity of carboxymethyl κ-carrageenan based green polymer electrolyte," *Solid State Ionics*, vol. 224, pp. 51–57, 2012.

[31] N. N. Mobarak, F. N. Jumaah, M. A. Ghani, M. P. Abdullah, and A. Ahmad, "Carboxymethyl carrageenan based biopolymer electrolytes," *Electrochimica Acta*, vol. 175, pp. 224–231, 2015.

[32] T. M. Di Palma, F. Migliardini, D. Caputo, and P. Corbo, "Xanthan and κ-carrageenan based alkaline hydrogels as electrolytes for Al/air batteries," *Carbohydrate Polymers*, vol. 157, pp. 122–127, 2017.

[33] A. S. A. Khiar and A. K. Arof, "Conductivity studies of starch-based polymer electrolytes," *Ionics*, vol. 16, no. 2, pp. 123–129, 2009.

[34] M. Kumar, T. Tiwari, and N. Srivastava, "Electrical transport behaviour of bio-polymer electrolyte system: potato starch+ammonium iodide," *Carbohydrate Polymers*, vol. 88, no. 1, pp. 54–60, 2012.

[35] M. F. Shukur, R. Ithnin, and M. F. Z. Kadir, "Electrical characterization of corn starch-LiOAc electrolytes and application in electrochemical double layer capacitor," *Electrochimica Acta*, vol. 136, pp. 204–216, 2014.

[36] D. Kotatha, K. Morishima, S. Uchida et al., "Preparation and characterization of gel electrolyte with bacterial cellulose coated with alternating layers of chitosan and alginate for electric double-layer capacitors," *Research on Chemical Intermediates*, vol. 44, no. 8, pp. 4971–4987, 2018.

[37] T. Furuike, T. Chaochai, T. Okubo, T. Mori, and H. Tamura, "Fabrication of nonwoven fabrics consisting of gelatin nanofibers cross-linked by glutaraldehyde or N-acetyl-d-glucosamine by aqueous method," *International Journal of Biological Macromolecules*, vol. 93, pp. 1530–1538, 2016.

[38] M. Peter, N. Ganesh, N. Selvamurugan et al., "Preparation and characterization of chitosan-gelatin/nanohydroxyapatite composite scaffolds for tissue engineering applications," *Carbohydrate Polymers*, vol. 80, no. 3, pp. 687–694, 2010.

[39] L. Ji, W. Qiao, Y. Zhang et al., "A gelatin composite scaffold strengthened by drug-loaded halloysite nanotubes," *Materials Science and Engineering: C*, vol. 78, pp. 362–369, 2017.

[40] X. Liu and P. X. Ma, "Phase separation, pore structure, and properties of nanofibrous gelatin scaffolds," *Biomaterials*, vol. 30, no. 25, pp. 4094–4103, 2009.

[41] M. B. Dainiak, I. U. Allan, I. N. Savina et al., "Gelatin-fibrinogen cryogel dermal matrices for wound repair: preparation, optimisation and in vitro study," *Biomaterials*, vol. 31, no. 1, pp. 67–76, 2010.

[42] F. Zhang, C. He, L. Cao et al., "Fabrication of gelatin-hyaluronic acid hybrid scaffolds with tunable porous structures for soft tissue engineering," *International Journal of Biological Macromolecules*, vol. 48, no. 3, pp. 474–481, 2011.

[43] T. Billiet, E. Gevaert, T. De Schryver, M. Cornelissen, and P. Dubruel, "The 3D printing of gelatin methacrylamide cell-laden tissue-engineered constructs with high cell viability," *Biomaterials*, vol. 35, no. 1, pp. 49–62, 2014.

[44] R. Ramadan, H. Kamal, H. M. Hashem, and K. Abdel-Hady, "Gelatin-based solid electrolyte releasing Li+ for smart window applications," *Solar Energy Materials and Solar Cells*, vol. 127, pp. 147–156, 2014.

[45] M. Khannam, R. Boruah, and S. K. Dolui, "An efficient quasi-solid state dye sensitized solar cells based on graphene oxide/gelatin gel electrolyte with NiO supported TiO_2 photoanode," *Journal of Photochemistry and Photobiology A: Chemistry*, vol. 335, pp. 248–258, 2017.

[46] Z. Tang, J. Wu, Q. Liu et al., "Preparation of poly(acrylic acid)/gelatin/polyaniline gel-electrolyte and its application in quasi-solid-state dye-sensitized solar cells," *Journal of Power Sources*, vol. 203, pp. 282–287, 2012.

[47] R. Leones, F. Sentanin, L. C. Rodrigues et al., "Novel polymer electrolytes based on gelatin and ionic liquids," *Optical Materials*, vol. 35, no. 2, pp. 187–195, 2012.

[48] D. F. Vieira, C. O. Avellaneda, and A. Pawlicka, "Conductivity study of a gelatin-based polymer electrolyte," *Electrochimica Acta*, vol. 53, no. 4, pp. 1404–1408, 2007.

[49] C. O. Avellaneda, D. F. Vieira, A. Al-Kahlout et al., "All solid-state electrochromic devices with gelatin-based electrolyte," *Solar Energy Materials and Solar Cells*, vol. 92, no. 2, pp. 228–233, 2008.

[50] H. Nagahama, H. Maeda, T. Kashiki, R. Jayakumar, T. Furuike, and H. Tamura, "Preparation and characterization of novel chitosan/gelatin membranes using chitosan hydrogel," *Carbohydrate Polymers*, vol. 76, no. 2, pp. 255–260, 2009.

[51] M. S. Rahman, G. Al-Saidi, N. Guizani, and A. Abdullah, "Development of state diagram of bovine gelatin by measuring thermal characteristics using differential scanning calorimetry (DSC) and cooling curve method," *Thermochimica Acta*, vol. 509, no. 1-2, pp. 111–119, 2010.

[52] X. Wang, B. Ding, and B. Li, "Biomimetic electrospun nanofibrous structures for tissue engineering," *Materials Today*, vol. 16, no. 6, pp. 229–241, 2013.

[53] X. Shi, W. Zhou, D. Ma et al., "Electrospinning of nanofibers and their applications for energy devices," *Journal of Nanomaterials*, vol. 2015, Article ID 140716, 20 pages, 2015.

[54] H. Niu and T. Lin, "Fiber generators in needleless electrospinning," *Journal of Nanomaterials*, vol. 2012, Article ID 725950, 13 pages, 2012.

[55] T. Chaochai, H. Miyaji, T. Nishida, T. Tamura, and H. au, "Preparation of chitosan-gelatin based sponge cross-linked with GlcNAc for bone tissue engineering," *Journal of Chitin and Chitosan Science*, vol. 4, no. 2, pp. 1–8, 2016.

[56] Y.-P. Wang, X.-H. Gao, R.-M. Wang, H.-G. Liu, C. Yang, and Y.-B. Xiong, "Effect of functionalized montmorillonite addition on the thermal properties and ionic conductivity of PVDF-PEG polymer electrolyte," *Reactive and Functional Polymers*, vol. 68, no. 7, pp. 1170–1177, 2008.

[57] S. Ambika and M. A. Sundrarajan, "[EMIM] BF4 ionic liquid-mediated synthesis of TiO2 nanoparticles using Vitex negundo Linn extract and its antibacterial activity," *Journal of Molecular Liquids*, vol. 221, pp. 986–992, 2016.

[58] T. Romann, O. Oll, P. Pikma, H. Tamme, and E. Lust, "Surface chemistry of carbon electrodes in 1-ethyl-3-methylimidazolium tetrafluoroborate ionic liquid - an in situ infrared study," *Electrochimica Acta*, vol. 125, pp. 183–190, 2014.

[59] V. S. Rao, T. V. Krishna, T. M. Mohan, and P. M. Rao, "Physicochemical properties of green solvent 1-ethyl-3-methylimidazolium tetrafluoroborate with aniline from T = (293.15 to 323.15) K at atmospheric pressure," *The Journal of Chemical Thermodynamics*, vol. 104, pp. 150–161, 2017.

[60] K. Jalaja, V. S. Sreehari, P. R. A. Kumar, and R. J. Nirmala, "Graphene oxide decorated electrospun gelatin nanofibers: fabrication, properties and applications," *Materials Science and Engineering: C*, vol. 64, pp. 11–19, 2016.

[61] D. M. Correia, J. Padrão, L. R. Rodrigues, F. Dourado, S. Lanceros-Méndez, and V. Sencadas, "Thermal and hydrolytic degradation of electrospun fish gelatin membranes," *Polymer Testing*, vol. 32, no. 5, pp. 995–1000, 2013.

[62] Y. Cao and T. Mu, "Comprehensive investigation on the thermal stability of 66 ionic liquids by thermogravimetric analysis," *Industrial and Engineering Chemistry Research*, vol. 53, no. 20, pp. 8651–8664, 2014.

[63] L. Lin, Y. Gu, and H. Cui, "Novel electrospun gelatin-glycerin-ε-poly-lysine nanofibers for controlling *Listeria monocytogenes* on beef," *Food Packaging and Shelf Life*, vol. 18, pp. 21–30, 2018.

[64] I. Mukherjee and M. Rosolen, "Thermal transitions of gelatin evaluated using DSC sample pans of various seal integrities," *Journal of Thermal Analysis and Calorimetry*, vol. 114, no. 3, pp. 1161–1166, 2013.

[65] H. W. Kwak, M. Shin, J. Y. Lee et al., "Fabrication of an ultrafine fish gelatin nanofibrous web from an aqueous solution by electrospinning," *International Journal of Biological Macromolecules*, vol. 102, pp. 1092–1103, 2017.

[66] M. B. Bazbouz, H. Liang, and G. Tronci, "A UV-cured nanofibrous membrane of vinylbenzylated gelatin-poly (ε-caprolactone) dimethacrylate co-network by scalable free surface electrospinning," *Materials Science and Engineering C*, vol. 91, pp. 541–555, 2018.

[67] M. Kharaziha, M. Nikkhah, S.-R. Shin et al., "PGS:gelatin nanofibrous scaffolds with tunable mechanical and structural properties for engineering cardiac tissues," *Biomaterials*, vol. 34, no. 27, pp. 6355–6366, 2013.

[68] D. Kotatha, Y. Torii, K. Shinomiya et al., "Preparation of thin-film electrolyte from chitosan-containing ionic liquid for application to electric double-layer capacitors," *International Journal of Biological Macromolecules*, vol. 124, pp. 1274–1280, 2019.

[69] X. Liu and T. Osaka, "Properties of electric double-layer capacitors with various polymer gel electrolytes," *Journal of The Electrochemical Society*, vol. 144, no. 9, pp. 3066–3071, 1997.

[70] C.-C. Yang, S.-T. Hsu, and W.-C. Chien, "All solid-state electric double-layer capacitors based on alkaline polyvinyl alcohol polymer electrolytes," *Journal of Power Sources*, vol. 152, pp. 303–310, 2005.

[71] A. Lewandowski and A. Świderska, "Electrochemical capacitors with polymer electrolytes based on ionic liquids," *Solid State Ionics*, vol. 161, no. 3-4, pp. 243–249, 2003.